ELSEVIER

Journal of Hepatology 46 (2007) 840–848

Journal of Hepatology

www.elsevier.com/locate/jhep

Vascular remodeling and antitumoral effects of mTOR inhibition in a rat model of hepatocellular carcinoma☆

David Semela[1], Anne-Christine Piguet[1], Mirjam Kolev[1], Karin Schmitter[1], Ruslan Hlushchuk[2], Valentin Djonov[2], Christoforos Stoupis[3], Jean-François Dufour[1,*]

[1]*Institute of Clinical Pharmacology, University of Berne, Murtenstrasse 35, CH-3010 Berne, Switzerland*
[2]*Institute of Anatomy, University of Berne, Berne, Switzerland*
[3]*Institute for Diagnostic Radiology, Inselspital Berne, Berne, Switzerland*

***Background/Aims*: Hepatocellular carcinoma (HCC) is amenable to only few treatments. Inhibitors of the kinase mTOR are a new class of immunosuppressors already in use after liver transplantation. Their antiproliferative and antiangiogenic properties suggest that these drugs could be considered to treat HCC. We investigated the antitumoral effects of mTOR inhibition in a HCC model.**

***Methods*: Hepatoma cells were implanted into livers of syngeneic rats. Animals were treated with the mTOR inhibitor sirolimus for 4 weeks. Tumor growth was monitored by MR imaging. Antiangiogenic effects were assessed *in vivo* by microvessel density and corrosion casts and *in vitro* by cell proliferation, tube formation and aortic ring assays.**

***Results*: Treated rats had significantly longer survival and developed smaller tumors, fewer extrahepatic metastases and less ascites than controls. Sirolimus decreased intratumoral microvessel density resulting in extensive necrosis. Endothelial cell proliferation was inhibited at lower drug concentrations than hepatoma cells. Tube formation and vascular sprouting of aortic rings were significantly impaired by mTOR inhibition. Casts revealed that in tumors treated with sirolimus vascular sprouting was absent, whereas intussusception was observed.**

***Conclusions*: mTOR inhibition significantly reduces HCC growth and improves survival primarily via antiangiogenic effects. Inhibitors of mTOR may have a role in HCC treatment.**

***Keywords*: Angiogenesis; Intussusception; Liver; Mammalian target of rapamycin; Sirolimus**

1. Introduction

There are more than half a million new cases of hepatocellular carcinoma (HCC) each year making it the fifth most common tumor worldwide and the third cause of cancer-related deaths [1]. The incidence of HCC is increasing and mortality has nearly doubled over the last 20 years [2]. Curative treatments such as liver resection and transplantation are only possible if the tumor is detected at an early stage [3]. Prognosis of HCC remains poor since only a minority of patients qualifies for these treatments. Systemic chemotherapy is not effective in HCC and local treatments such as chemoembolization have shown only limited survival benefit in selected patients [3]. Innovative therapeutic approaches are urgently needed.

HCC displays a characteristic hypervascularity and depends on angiogenesis for tumor growth [4]. Intratumoral microvessel density (MVD) is a predicting factor of disease-free survival after curative resection

Received 27 June 2006; received in revised form 26 September 2006; accepted 2 November 2006; available online 17 January 2007

☆ The authors who have taken part in this study declared that they have not a relationship with the manufacturers of the drugs involved either in the past or present and did not receive funding from the manufacturers to carry out their research. The authors did not receive funding from any source to carry out this study.

* Corresponding author. Tel.: +41 31 632 31 91; fax: +41 31 632 49 97.

E-mail address: jf.dufour@ikp.unibe.ch (J.-F. Dufour).

0168-8278/$32.00
doi:10.1016/j.jhep.2006.11.021

of HCC [5]. A prospective study with HCC patients found that high serum levels of vascular endothelial growth factor (VEGF), the most important growth factor for endothelial cells, are associated with absence of a tumor capsule, with tumor invasion and postoperative recurrence [6].

Recently, Geissler and coworkers reported that pharmacological inhibition of the kinase mammalian target of rapamycin (mTOR) with sirolimus (rapamycin) impairs tumor growth by an antiangiogenic mechanism. Sirolimus was shown to inhibit VEGF secretion and VEGF signaling in endothelial cells [7]. mTOR is a highly conserved serine–threonine kinase and plays a central role in modulating cell growth and proliferation [8]. In response to cellular nutritional status and activation of the upstream PI-3 kinase/Akt pathway, mTOR enhances mRNA translation and protein synthesis by phosphorylating its downstream targets p70 S6 kinase (S6K) and the translation initiation factor 4E-binding protein 1 (4E-BP1) [9]. Inhibition of mTOR induces arrest of the cell cycle in G1 phase [10] and interrupts downstream propagation of PI-3 kinase/Akt-mediated proliferative signals [7]. mTOR-dependent signaling was found to be activated in several tumor types including HCC [11,12]. Immunohistochemical studies revealed that 45% of HCC displayed an increased expression of S6K which correlates with tumor nuclear grade whereas hepatic adenomas did not have increased S6K expression [11].

The immunosuppressive drugs, sirolimus (rapamycin), temsirolimus (CCI-779) and everolimus, are inhibitors of mTOR and possess antiproliferative and antiangiogenic properties [12]. These drugs are currently being evaluated in clinical trials for various malignancies [12], but not yet for HCC. We tested the antitumoral properties of mTOR inhibition in a HCC model and investigated the antiangiogenic effects of this treatment. Our results provide the first *in vivo* data in HCC and a rationale to test pharmacological mTOR inhibition in patients with HCC.

2. Materials and methods

2.1. Cells and culture conditions

Morris Hepatoma McA-RH7777 (MH) cells were obtained from the German Cancer Research Center (DKFZ; Heidelberg, Germany) and were cultured in RPMI 1640 medium supplemented with 20% fetal bovine serum, L-glutamine, penicillin and streptomycin. Rat aortic endothelial cells were isolated from thoracic aorta of ACI rats by collagenase and cultured in F12-K medium (Gibco, Basel, Switzerland) with 10% fetal bovine serum (Sigma–Aldrich Chemie GmbH, Munich, Germany), penicillin and streptomycin, supplemented with 10 ng/ml epidermal growth factor and 25 μg/ml heparin. Endothelial cells were cultured on fibronectin coated wells (10 μg/ml, BD Biosciences, Allschwil, Switzerland) and were used between passages 1 and 6.

2.2. Animals

Experiments were performed in 12–18 weeks old ACI rats (Harlan, Indianapolis, USA). Animals received humane care in accordance with the regulations for laboratory animals and the experiments were approved by the Local Animal Use Committee.

2.3. Tumor implantation and treatment with sirolimus

Subcutaneously injected MH cells (5×10^6) in a syngeneic ACI rat led to formation of a subcutaneous tumor within 14 days. Tumor inocula were prepared by mincing the excised subcutaneous tumor into equal cubes of 1 mm^3. One single cube per rat was then immediately surgically implanted in the liver [13]. Rats were anaesthetized by intraperitoneal injection of medetomid 0.15 mg/kg, climazolam 2 mg/kg, and fentanyl 5 ng/kg. A subxyphoid incision was performed and a small superficial incision of the liver capsule allowed placement of a single 1 mm^3 tumor cube into the parenchyma (Fig. 1). After randomization, treatment with sirolimus was started on day 5 posttumor implantation. Treated rats were separated in single cages and received 2 mg sirolimus/kg body weight per day mixed in drinking water vs. drinking water without sirolimus in controls. Sirolimus solution was kept in light protected bottles and renewed every 48 h. The amount of ingested water and sirolimus per rat was monitored and kept at 2 mg sirolimus/kg body weight/day for 4 weeks. Rats were euthanized on day 33 after tumor implantation. In a separate series for survival analysis, animals were euthanized if they became wasted and seemed to be suffering (hunch-back posture) as assessed by a person unaware of treatment assignment. Serum, whole blood, tumors and livers were harvested. Tumor volume was calculated *ex vivo* (tumor volume = $4/3 \times \pi \times r_1 \times r_2 \times r_3$).

2.4. MR imaging

MR imaging was performed on day 17 after tumor implantation and weekly thereafter with a 1.5 T Sonata MRI unit (Siemens, Erlangen, Germany) using a high-resolution wrist phased array coil. Contiguous, 1-mm thick slices in axial plane were acquired using non-enhanced 3D T1 (VIBE, TR = 10 ms, TE = 3.71 ms, voxel size $0.5 \times 0.4 \times 1$ mm) and 3D T2 (3D turbo spin echo sequence for isotope resolution TR 3200 ms, TE 113 ms, voxel size $0.4 \times 0.4 \times 1.0$ mm) weighted sequences. Tumors were seen as demarcated areas of low signal intensity in T1 and high signal intensity in T2 weighted images, compared to the normal hepatic parenchyma.

2.5. Sirolimus level

Sirolimus whole blood levels were measured at harvest by high-performance liquid chromatography.

2.6. Tumor necrosis

Central tumor necrosis, characterized by macroscopic demarcation of the necrotic areas from the surrounding viable tumor tissue, was assessed by cutting the tumor at its largest diameter in half and measuring the largest diameter and the corresponding perpendicular diameter (x, y) of the macroscopically visible central necrosis. The radius of the tumor (r_{tumor}) and of the central necrotic zone (r_{necrosis}) was calculated for a hypothetical circle with the same surface as the ellipse formed by the two measured perpendicular diameters x and y.

2.7. Microvessel density

A monoclonal antibody against the endothelial cell antigen CD31 (clone JC/70 A, Dako, Glostrup, Denmark) was used at 1:150 dilution to mark the vessels. Microvessel density was determined blindly as described by Weidner and Folkman [14].

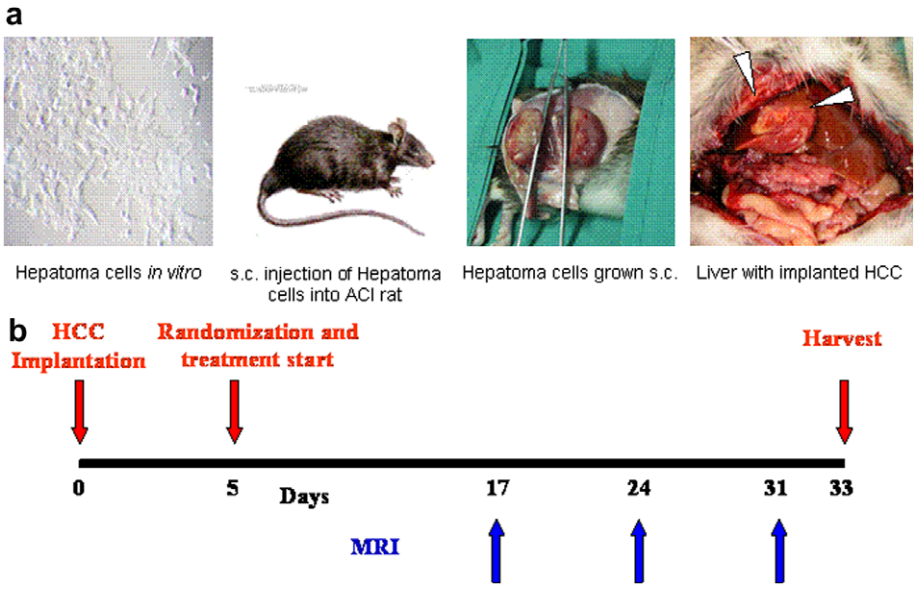

Fig. 1. ***In vivo*** **study design. (a) Subcutaneous injection of Morris hepatoma (MH) cells in a syngeneic ACI rat led to formation of a tumor within 14 days. The subcutaneous tumor was excised and equal cubes of 1 mm^3 were prepared. A single tumor cube per animal was immediately implanted into livers of ACI rats (arrowheads showing HCC growing in liver after two weeks). (b) Animals were randomized 5 days after HCC implantation and treatment for 4 weeks was started (sirolimus 2 mg/day/kg po vs. controls). HCC growth was monitored weekly by liver MR imaging starting on day 17 posttumor implantation. Rats were euthanized on day 33 after tumor implantation (corresponding 4 weeks of treatment). [This figure appears in colour on the web.]**

2.8. Immunoblot analysis

Tissue parts were minced and homogenized in 0.25 M sucrose (Polytron; Janke&Kunken KG IGA Werk, Staufen, Germany). Protein concentration was determined according to Lowry [15]. Proteins were separated using a 15% polyacrylamide gel and transferred to Protean nitro-cellulose membranes. Membranes were probed with an anti-phospho-4E-BP1 antibody 1:1000 (Cell Signaling #9455, Beverly MA, USA), incubated with secondary anti-rabbit IgG-coupled HRP antibody 1:50,000 (Pierce, Lausanne, Switzerland) and

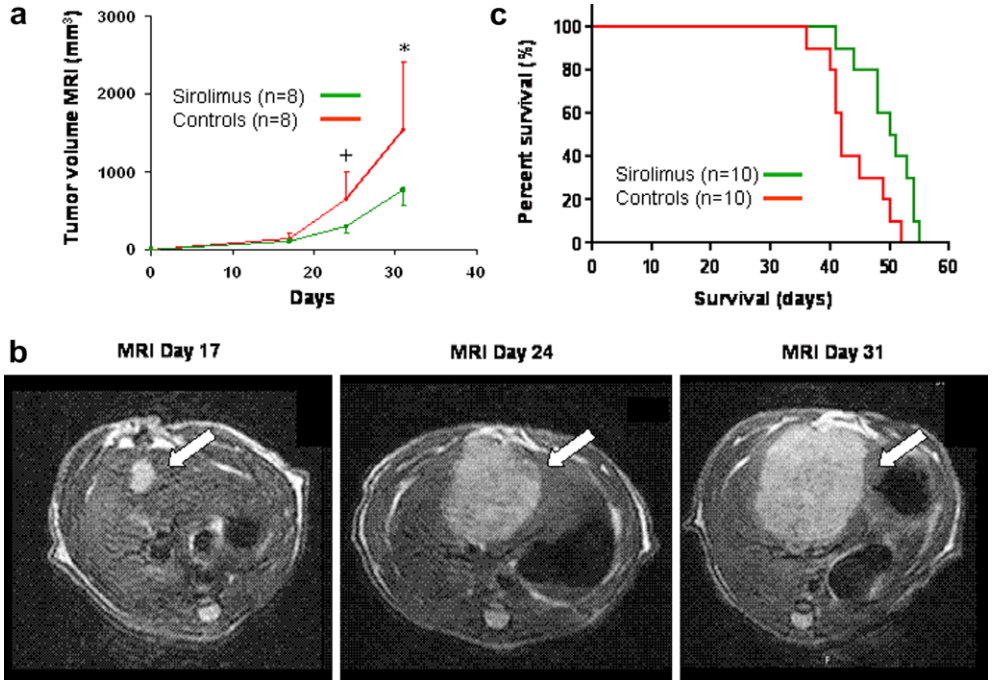

Fig. 2. Sirolimus inhibits HCC growth *in vivo*. (a) MR imaging revealed that the tumor volume was significantly lower on day 24 and 31 in the treated group in comparison to controls ($^+p < 0.004$ and $^*p < 0.01$, respectively; $n = 8$ in each group). (b) Liver MRI of the same tumor-bearing control animal was performed on days 17, 24 and 31 as shown on these three representative T2 weighed images showing growing HCC (arrow). (c) The effect of sirolimus on survival was studied in a second set of experiments: mean survival of controls ($n = 10$) was 42.0 days vs. 50.5 days in treated rats ($n = 10$) ($p = 0.0122$). [This figure appears in colour on the web.]

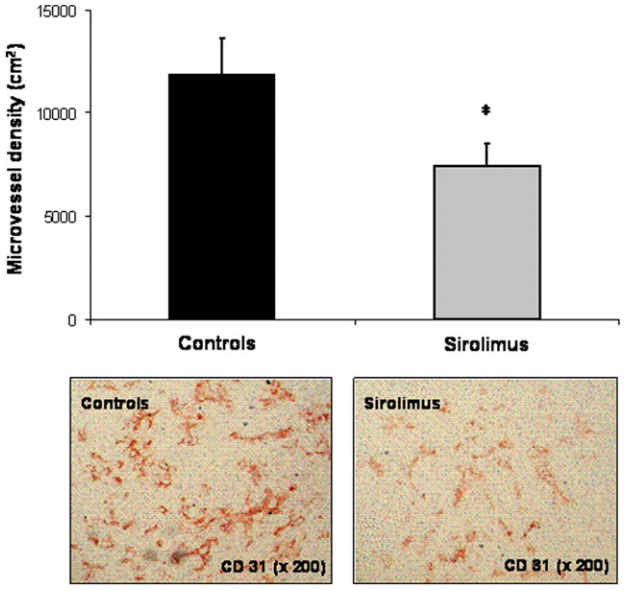

Fig. 3. Sirolimus has *in vivo* antiangiogenic effects. Intratumoral microvessel density (MVD) is decreased in animals treated with sirolimus. The degree of angiogenesis in tumor specimens was quantified by measuring MVD using a monoclonal antibody against the endothelial cell antigen CD31 on paraffin sections of tumor tissue (magnification 200×). Quantification of MVD per cm^2 reveals a significant decrease in rats treated with sirolimus (‡$p < 0.02$). [This figure appears in colour on the web.]

subjected to enhanced chemiluminescence (Perkin-Elmer, Zaventen, Belgium). Membranes were stripped and re-probed with anti-actin antibody 1:1000 (Sigma–Aldrich Chemie GmbH, Munich, Germany).

2.9. Capillary tube formation assay

Isolated rat aortic endothelial cells were seeded in slide chambers (Lab-Tek Chamber Slide, Nunc, Wiesbaden, Germany) coated with Matrigel (BD Biosciences, Allschwil, Switzerland). Temsirolimus, a soluble prodrug of sirolimus, which was provided by Wyeth Pharmaceuticals AG (Zug, Switzerland), was added to the wells. After 72-h, endothelial cells were fixed and stained using a Diff-Quick solution II staining protocol (Diff-Quick Stain Set; Baxter-Dade AG Duedingen, Switzerland). The length of vascular tubes was measured at 40× magnification with Scion image (Scion Corp, NIH, Beta 4.0.2) and expressed as vascular surface [16]. All assays were performed in triplicate in three independent experiments.

2.10. Aortic ring assay

Thoracic aortas excised from 8- to 12-week-old ACI rats (range 180–230 g) were cut into 1-mm-long cross-sections. Rings were placed on Matrigel-coated wells with F12-K medium (Gibco, Basel, Switzerland) with 10% fetal bovine serum (Sigma–Aldrich Chemie GmbH, Munich, Germany), penicillin, streptomycin and supplemented with 10 ng/ml epidermal growth factor and 25 μg/ml heparin. Temsirolimus was added. As controls, complete medium with vehicle was assayed. After 5 days, rings were fixed and stained using a Diff-Quick solution II staining protocol (Diff-Quick Stain Set; Baxter-Dade AG Duedingen, Switzerland). Vascular outgrowth was quantified by counting all sprouts from one ring. All assays were performed in triplicate and each experiment was repeated three times.

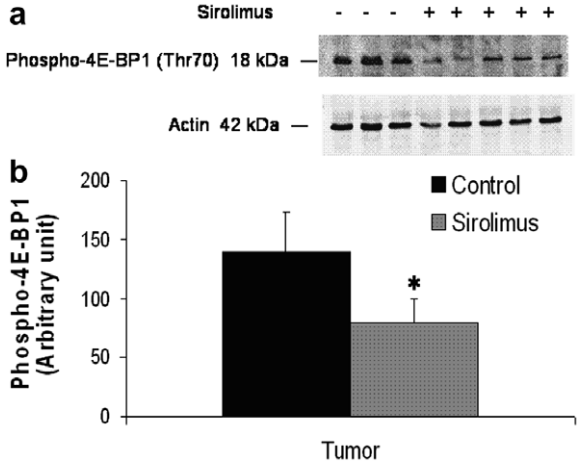

Fig. 4. Effect of sirolimus on hepatic phosphorylation of 4E-BP1 in HCC tissue. (a) The top panel shows a representative immunoblot of phosphorylated 4E-BP1 in HCC tissue and the lower panel the same membrane after stripping and reprobing with an anti-actin antibody. (b) Quantification of the immunoblots revealed significantly less phosphorylation of 4E-BP1 after inhibition of mTOR in HCC tissue of animals treated with sirolimus (*$p < 0.001$, $n = 8$).

2.11. Chorio-allantoic membrane assay

Twenty microliters of temsirolimus solution at the final concentrations of 0.1–1000 ng/ml was applied on shell-free chicken chorio-allantoic membranes as previously described [17]. Twenty-four hours later the chorio-allantoic membranes were examined after intravascular injection of 0.1 ml of 2.5% fluorescein isothiocyanate dextran 2000 kDa (Sigma–Aldrich Chemie Gmbh, Munich, Germany). Vessels were visualized by fluorescence microscopy and microvascular patterns were monitored using an LE CCD Optronics video camera (Visitron System, Puchheim, Germany).

2.12. Thymidine incorporation assay

Cells were incubated for 20 h with temsirolimus at concentrations ranging from 1 to 1000 ng/ml in presence of 2 μCi/ml [^{3}H] thymidine (10 mCi/ml, Sigma–Aldrich Chemie Gmbh, Munich, Germany). After removal of the medium, cells were rinsed with ice-cold 5% trichloroacetic acid and were solubilized by shaking in 0.4 M NaOH. Incorporated radioactivity was measured by scintillation counting. Each experiment was performed three times in triplicate. Identical experiments were performed for the HCC cell lines HepG2, Hep3B, and HuH7.

2.13. Flow cytometry

After 6 h of incubation (temsirolimus 0.1–1000 ng/ml or vehicle), MH cells and endothelial cells were harvested and labeled with FITC-conjugated Annexin V and propidium iodide (MBL, LabForce, Nunnigen, Switzerland). A Becton–Dickinson BD FacScan flow cytometer was used to quantify Annexin V positive propidium iodide negative apoptotic cells.

2.14. Realtime quantitative PCR

Total RNA was extracted from tumor samples as described [18]. RNA was treated by DNase digestion (RQ1 RNAse-free DNase, Promega, Mannheim, Germany) and reverse-transcribed with MMLV reverse transcriptase (Gibco–BRL, Basel, Switzerland) with a random hexanucleotide mix. Specific forward and reverse primers as well as the fluorogenic probes were designed according to Perkin-Elmer guidelines

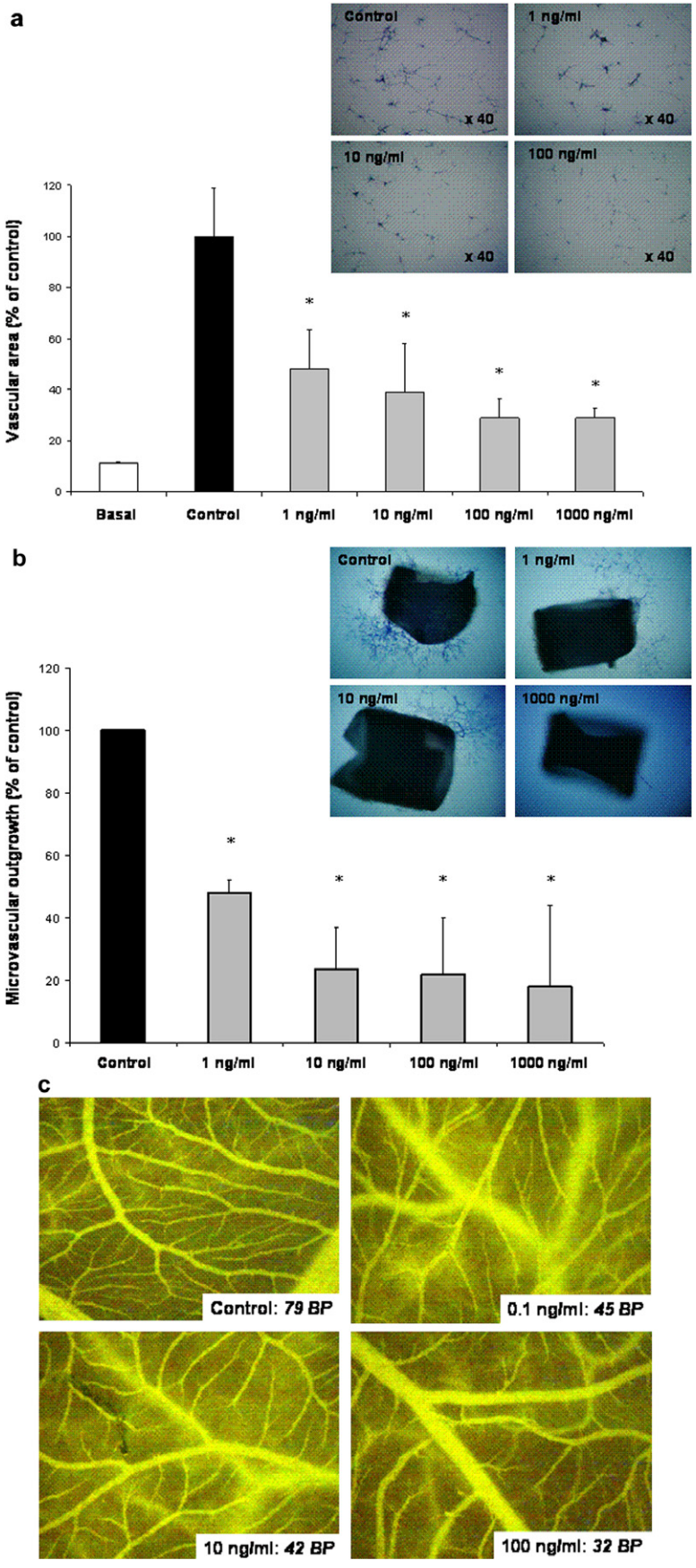
a
Control
1 ng/ml
10 ng/ml
100 ng/ml
x 40
Vascular area (% of control)
120
100
80
60
40
20
0
*
Basal
Control
1 ng/ml
10 ng/ml
100 ng/ml
1000 ng/ml
b
Control
1 ng/ml
10 ng/ml
1000 ng/ml
Microvascular outgrowth (% of control)
120
100
80
60
40
20
0
*
Control
1 ng/ml
10 ng/ml
100 ng/ml
1000 ng/ml
c
Control: 79 BP
0.1 ng/ml: 45 BP
10 ng/ml: 42 BP
100 ng/ml: 32 BP

(Primer Express Software) and were tested for optimal concentration and linear amplification before beginning quantitative measurements. The primers and probe were: *VEGF165*: AGTCCAACATCA CCATGCAGATTA and GCATTCACATTTGTTGTGCTGTAG with the probe CCTCACCAAGGCCAGCACATAGGAGA.

Quantitative assessment of mRNA expression was performed using 18S ribosomal RNA as an internal standard (Applied Biosystems). Δ(Ct) represents the difference in number of PCR cycles to reach the same fluorescent intensity.

2.15. Vascular casting

As previously described [19], the liver vasculature was perfused with a freshly prepared solution of Mercox® (Vilene Company, Japan) containing 0.1 ml of accelerator per 5 ml of resin. One hour after perfusion, the tumors were excised and transferred to 15% potassium hydroxide for maceration. After 3–4 weeks, the casts were washed and dehydrated in ethanol and dried in a vacuum desiccator. Samples were layered with gold to a thickness of 10 nm and examined in a Philips XL 30 FEG scanning electron microscope.

2.16. Statistical analysis

Data points are given as mean values ± standard deviations. Statistical significance was determined by non-parametric tests: Kurskal–Wallis ANOVA and Mann–Whitney *U* test. Difference in survival was measured by the log-rank test. A value of $p < 0.05$ was considered significant.

3. Results

All rats ($n = 8$/group) developed HCC and finished 4 weeks of treatment (Fig. 1). Animals treated with sirolimus developed significantly smaller tumors than untreated animals as assessed by repetitive MR imaging (Fig. 2a and b). Tumor sizes before harvest after 4 weeks of treatment were 775 $mm^3 \pm 214$ in the sirolimus treated group and 1538 $mm^3 \pm 884$ in the control group ($p < 0.05$). Survival was significantly longer in treated animals than in controls (mean survival 50.5 vs. 42.0 days; $p = 0.0122$, $n = 10$/group) (Fig. 2c). Macroscopic measurement of central necrosis showed that the mean tumor diameter in rats treated with sirolimus was not only smaller (7.1 ± 0.3 mm vs. 8.6 ± 1.5 mm; $p = 0.036$), but that the size of the central necrosis as a parameter of antiangiogenic effectiveness was also larger (224 ± 77 mm^3 vs. 149 ± 144 mm^3). Moreover, 25% of the control animals had sero-sanguinous ascites at harvest, whereas none of sirolimus treated animals did. Immunohistological analysis revealed a significant decrease of MVD in sirolimus treated rats (Fig. 3). At harvest the mean whole blood level of sirolimus was 0.7 ng/ml. Immunoblotting found that the mTOR substrate 4E-BP1 was less phosphorylated in treated

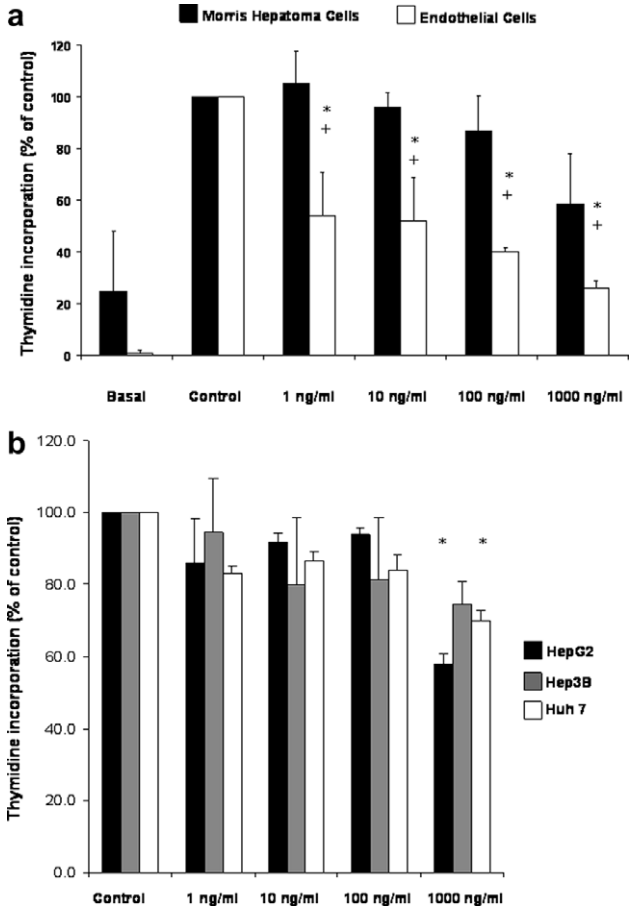

Fig. 6. Endothelial cell proliferation is selectively blocked at low concentrations of temsirolimus. (a) Cell proliferation of isolated aortic endothelial cells and MH cells was measured by incorporation of [^{3}H] thymidine as described in Section 2. Each experiment was performed three times (*$p < 0.05$ in comparison to MH cells at given temsirolimus concentration and $^+p < 0.05$ in comparison to endothelial cell control). (b) Cell proliferation measured by thymidine incorporation of the HCC cell lines HepG2, Hep3B, and HuH7. Each experiment was performed three times (*$p < 0.05$ Kurskal–Wallis ANOVA).

Fig. 5. mTOR inhibition blocks blood vessel formation *in vitro* and *in vivo*. (a) The mTOR inhibitor temsirolimus inhibits capillary tube formation of endothelial cells on Matrigel at ⩾1 ng/ml. Rat aortic endothelial cells were isolated and incubated on Matrigel with various concentrations of temsirolimus (1, 10, 100 and 1000 ng/ml). Endothelial cells were fixed and stained after 72 h of incubation. Each well was photographed at random and compared to controls incubated in complete medium with vehicle and to FBS-free medium (Basal) (magnification 40×). Areas covered with vascular tubes were digitally quantified using the software Scion image (Scion Corp, NIH, Beta 4.0.2) and expressed as vascular surface corresponding to the number of pixels per photographed field. Results are expressed as percentage of controls incubated in complete medium without temsirolimus (*$p < 0.05$ in comparison to control). (b) Temsirolimus blocks sprouting of capillaries from rat aortic rings at concentrations ⩾1 ng/ml. Aortic rings from ACI rats were incubated in Matrigel and medium with or without temsirolimus at concentrations of 1, 10, 100 and 1000 ng/ml. After 5 days of incubation rings were fixed, stained and photographed. Vascular outgrowth was quantified by counting all capillary sprouts from one ring and normalized to controls (*$p < 0.05$ in comparison to control). (c) Chorio-allantoic membrane assay after intravascular injection of fluorescein isothiocyanate dextran (2000 kDa) to visualize the vessels (magnification 32×). Inhibition of mTOR for 24 h by application of temsirolimus on the chorio-allantoic membrane reduced in a dose-dependent manner the number of vascular branching points (BP). All four pictures have been taken at the same magnification (32×). [This figure appears in colour on the web.]

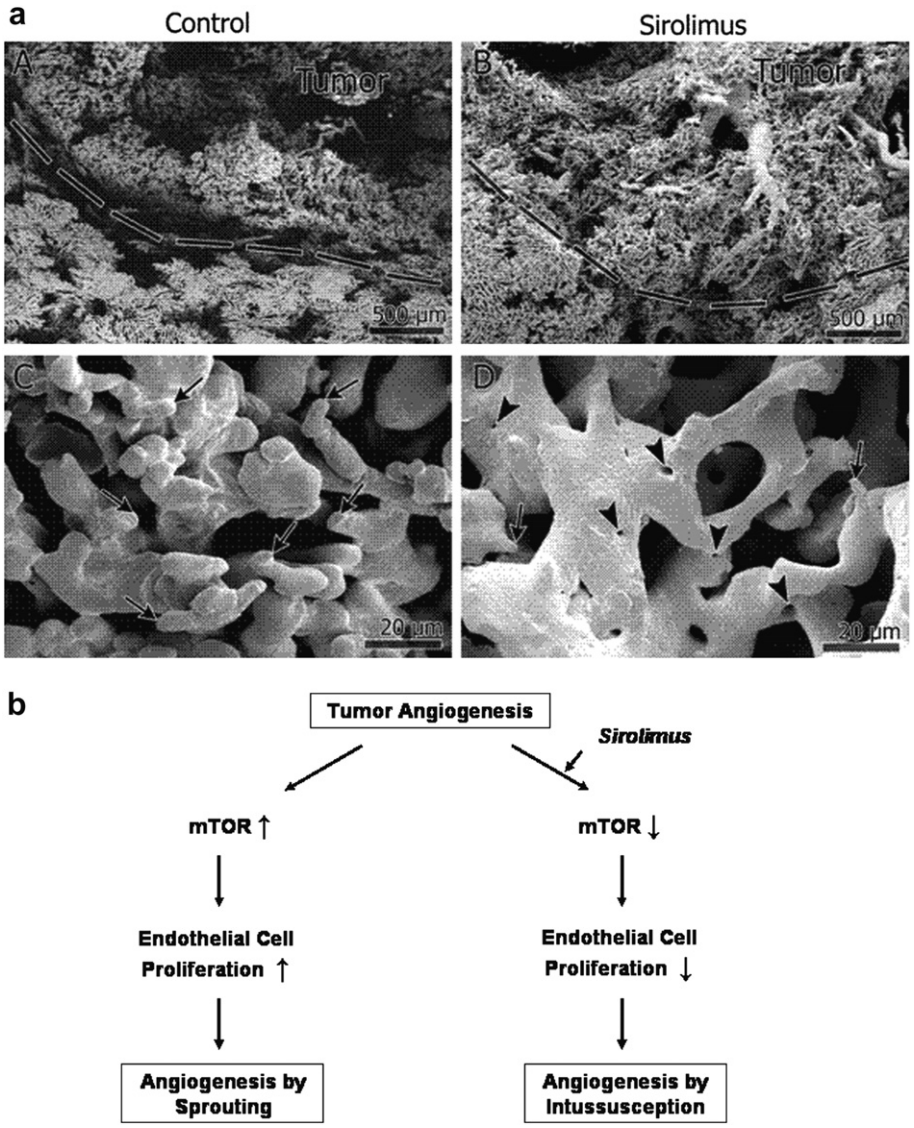

Fig. 7. Sirolimus inhibits vascular sprouting in tumor vessels. (a) Scanning electron microscopy of vascular casts shows tumor vasculature above the line (Tumor), whereas normal liver with sinusoidal microvasculature is shown in the lower half (A and B). In control animals the capillary plexus in tumor expanded predominantly by sprouting (C, arrows), which is formation of new blood vessels from a preexisting vascular bed by endothelial cell proliferation and subsequent lumen formation in the sprout. In contrast, sprouting was inhibited in animals treated with sirolimus and the main vascular growth mode in these animals was intussusception (D), which is a form of angiogenesis based on microvascular remodeling by transluminal pillar formation. Arrowheads indicate transluminal tissue pillars, which appear as holes in the casts and are exemplary for intussusception. (b) Schematic representation of findings in (a): unopposed tumor angiogenesis is based on proliferating endothelial cells in tumors, which lead to formation of new vessels by sprouting. Inhibition of the kinase mTOR by inhibitors of mTOR such as sirolimus blocks endothelial cell proliferation, whereby sprouting is replaced by intussusceptive angiogenesis.

animals than in controls (Fig. 4). mRNA levels of *VEGF* were lower in tumor tissue of treated rats than in tumor tissue of control rats (sirolimus $\Delta(\mathrm{Ct}) = 9.59 \pm 0.35$ $(n = 8)$ vs. controls $\Delta(\mathrm{Ct}) = 8.73 \pm 1.21$ $(n = 7)$, $p < 0.05$).

In vitro experiments were performed with the more hydrophilic temsirolimus, an ester prodrug, which is rapidly metabolized into sirolimus [12]. Tube formation assay showed significant inhibition of endothelial cells at temsirolimus concentrations $\geqslant 1$ ng/ml (Fig. 5a). Sprouting of capillaries from aortic rings, which involves proliferation and migration of smooth muscle cells and fibroblasts in addition to endothelial cells, was also inhibited at temsirolimus concentrations $\geqslant 1$ ng/ml (Fig. 5b). Confirmatory results were found using the chick chorioallantoic assay with a significant reduction in vessel length and branching points (Fig. 5c). Temsirolimus significantly inhibited thymidine incorporation in endothelial cells in a dose-dependent manner already at low doses of 1 ng/ml, whereas the MH cells were only inhibited at 1000 ng/ml (Fig. 6a). This result was confirmed in other HCC cell lines (HepG2, Hep3B and Huh7) (Fig. 6b). No increased rate of apoptosis analyzed by FACS analysis (% induced Annexin V positive cells after 6 h of

incubation) was seen in either vascular endothelial cells or MH cells for temsirolimus concentrations of up to 1000 ng/ml (results not shown).

Analysis of the tumoral vasculature by scanning electron microscopy of corrosion casts demonstrated a less fine vascular architecture in case of sirolimus treatment (Fig. 7A vs. B) and suggested that the mode of formation of new blood vessels was different in treated animals. Whereas the capillary plexus expanded primarily by sprouting in the control animals (Fig. 7C), this mechanism was nearly absent in the tumors of treated animals and replaced by intussusception as shown by the formation of numerous transcapillary pillars (Fig. 7D).

4. Discussion

Our results show that mTOR inhibition prevents the progression of HCC and improves survival. In this orthotopic, syngeneic model, rats treated with sirolimus had slower HCC growth, less metastases and less ascites than untreated animals. Histological examination revealed decreased intratumoral MVD and larger areas of central necrosis in animals receiving sirolimus. Inhibition of mTOR primarily affected proliferation of endothelial cells rather than proliferation of the malignant cells and blocked angiogenesis indicated by multiple assays providing an explanation for its mode of action.

Several mechanisms may account for the antiangiogenic effect of mTOR inhibitors such as sensitization of endothelial cells to apoptosis [20], thrombosis of the tumoral vascular bed [21] and inhibition of the differentiation of endothelial progenitor cells [22]. We did not observe apoptosis nor thrombosis. Our data suggest that the most likely mechanism was inhibition of endothelial cell proliferation and vascular sprouting. In contrast to endothelial cells, malignant MH cells were resistant to mTOR inhibition showing no significant inhibition of proliferation at concentrations below 1000 ng/ml, which is consistent with concentrations required in other HCC (Fig. 6b) and non-HCC tumor cell lines [23]. Moreover, vascular sprouting from aortic rings, which also involves supportive cells such as vascular smooth muscle cells and pericytes, was affected at comparable concentrations as per the endothelial cell capillary tube formation assay, which relies on endothelial cells alone. A similar observation was made with the chorio-allantoic membrane assay where the decrease in vessel length and number of branching points was present already at the lowest dose tested (0.1 ng/ml). These results suggest that, in addition to endothelial cells, mTOR inhibition may impair angiogenesis by affecting supportive cells of the vessel wall such as smooth muscle cells and pericytes [24].

In line with these experiments, analysis of tumor vasculature in sirolimus treated animals by scanning electron microscopy revealed inhibition of vessel formation by sprouting, which is the classical formation of new blood vessels from a preexisting vascular bed and is dependent on endothelial cell proliferation with subsequent lumen formation in the sprout. Sprouting in treated animals was replaced by angiogenesis via intussusception, which represents a different vascular growth pattern. In contrast to sprouting, angiogenesis by intussusception consists of microvascular remodeling by transcapillary pillar formation and relies much less on endothelial cell proliferation [17]. Growth of these endothelial pillars leads to new vessels by partitioning of the existing vascular lumen. Intussusceptive angiogenesis has been found in tumors to co-exist with sprouting [25–27]. A switch from sprouting to intussusceptive angiogenesis as mechanism of resistance of tumor vasculature to antiangiogenic treatment has not yet been described.

Dosing of sirolimus is critical to achieve maximal inhibition of angiogenesis in tumors. Best antiangiogenic effects were observed by maintaining low doses of sirolimus on a constant basis rather than by intermittent bolus administration [28]. In our experiments, we attempted a continuous basal exposure and sirolimus whole blood concentrations were measured below 1 ng/ml. This concentration is lower than the trough levels used for immunosuppression after transplantation. However, treated animals displayed not only a decrease in MVD but also a significant reduction in 4E-BP1 phosphorylation and in VEGF mRNA levels indicating that sirolimus was active *in vivo* at this dosage. Underphosphorylation of mTOR substrates interferes with crucial oncogenic pathways by impairing the translation of mRNA transcripts coding for VEGF, HIF and Myc [23,29]. Decreased expression of VEGF, as we found as well as others [7,30,31], might explain the reduced number of metastasis as well as the lack of ascites in the treated animals.

Sirolimus administration prolonged the survival of HCC-bearing animals, but failed to cure them. The corrosion casts revealed that angiogenesis was not completely blocked, but could occur by intussusception suggesting that this alternate mechanism is less dependent on mTOR and might help tumors to escape antiangiogenic treatment. One can therefore speculate that mTOR inhibitors would achieve better antitumoral effects when combined with a cytotoxic drug.

In summary, our results provide evidence that inhibition of mTOR blocks tumor angiogenesis, induces vascular remodeling and impairs HCC growth. Accordingly, treatment of HCC and prevention of HCC recurrence after liver transplantation are potential indications for mTOR inhibitors. These warrant further investigation in clinical trials.

Acknowledgements

We thank M. Ledermann for expert technical assistance in tissue handling and immunohistochemistry, K. Matozan and Dr. R. Rieben for endothelial cell isolation, F. Theiler for MR imaging and Dr. C. Redaelli for animal surgery. We are indebted to Drs. M. Schneider and C. Winnips (Wyeth Pharmaceuticals AG) for their interest in these experiments and for providing temsirolimus.

Financial support: This work was supported by the Bernische Krebsliga, the Stanley Thomas Johnson Foundation, the Swiss Society of Internal Medicine and the Swiss National Foundation Grant No. 3100-063696 to D.S.

References

[1] Parkin DM, Bray F, Ferlay J, Pisani P. Estimating the world cancer burden: Globocan 2000. Int J Cancer 2001;94:153–156.
[2] El-Serag HB, Davila JA, Petersen NJ, McGlynn KA. The continuing increase in the incidence of hepatocellular carcinoma in the United States: an update. Ann Intern Med 2003;139:817–823.
[3] Llovet JM. Treatment of hepatocellular carcinoma. Curr Treat Opt Gastroenterol 2004;7:431–441.
[4] Semela D, Dufour JF. Angiogenesis and hepatocellular carcinoma. J Hepatol 2004;41:864–880.
[5] Sun HC, Tang ZY, Li XM, Zhou YN, Sun BR, Ma ZC. Microvessel density of hepatocellular carcinoma: its relationship with prognosis. J Cancer Res Clin Oncol 1999;125:419–426.
[6] Poon RT, Ng IO, Lau C, Zhu LX, Yu WC, Lo CM, et al. Serum vascular endothelial growth factor predicts venous invasion in hepatocellular carcinoma: a prospective study. Ann Surg 2001;233:227–235.
[7] Guba M, von Breitenbuch P, Steinbauer M, Koehl G, Flegel S, Hornung M, et al. Rapamycin inhibits primary and metastatic tumor growth by antiangiogenesis: involvement of vascular endothelial growth factor. Nat Med 2002;8:128–135.
[8] Fingar DC, Blenis J. Target of rapamycin (TOR): an integrator of nutrient and growth factor signals and coordinator of cell growth and cell cycle progression. Oncogene 2004;23:3151–3171.
[9] Huang S, Bjornsti M, Houghton P. Rapamycins: mechanism of action and cellular resistance. Cancer Biol Ther 2003;2:222–232.
[10] Fingar DC, Richardson CJ, Tee AR, Cheatham L, Tsou C, Blenis J. mTOR controls cell cycle progression through its cell growth effectors S6K1 and 4E-BP1/eukaryotic translation initiation factor 4E. Mol Cell Biol 2004;24:200–216.
[11] Sahin F, Kannangai R, Adegbola O, Wang J, Su G, Torbenson M. mTOR and P70 S6 kinase expression in primary liver neoplasms. Clin Cancer Res 2004;10:8421–8425.
[12] Rao R, Buckner J, Sarkaria J. Mammalian target of rapamycin (mTOR) inhibitors as anti-cancer agents. Curr Cancer Drug Targets 2004;4:621–635.
[13] Yang R, Rescorla F, Reilly C, Faught P, Sanghvi N, Lumeng L, et al. A reproducible rat liver cancer model for experimental therapy: introducing a technique of intrahepatic tumor implantation. J Surg Res 1992;52:193–198.
[14] Weidner N, Semple JP, Welch WR, Folkman J. Tumor angiogenesis and metastasis – correlation in invasive breast carcinoma. N Engl J Med 1991;324:1–8.
[15] Lowry O, Rosebrough N, Farr L, Randall R. Protein measurement with the folin phenol reagent. J Biol Chem 1951;193:265–275.
[16] Grant DS, Kinsella JL, Fridman R, Auerbach R, Piasecki BA, Yamada Y, et al. Interaction of endothelial cells with a laminin A chain peptide (SIKVAV) in vitro and induction of angiogenic behavior in vivo. J Cell Physiol 1992;153:614–625.
[17] Djonov V, Schmid M, Tschanz SA, Burri PH. Intussusceptive angiogenesis: its role in embryonic vascular network formation. Circ Res 2000;86:286–292.
[18] Dufour JF, Luthi M, Forestier M, Magnino F. Expression of inositol 1,4,5-trisphosphate receptor isoforms in rat cirrhosis. Hepatology 1999;30:1018–1026.
[19] Djonov VG, Kurz H, Burri PH. Optimality in the developing vascular system: branching remodeling by means of intussusception as an efficient adaptation mechanism. Dev Dyn 2002;224:391–402.
[20] Bruns CJ, Koehl GE, Guba M, Yezhelyev M, Steinbauer M, Seeliger H, et al. Rapamycin-induced endothelial cell death and tumor vessel thrombosis potentiate cytotoxic therapy against pancreatic cancer. Clin Cancer Res 2004;10:2109–2119.
[21] Guba M, Yezhelyev M, Eichhorn ME, Schmid G, Ischenko I, Papyan A, et al. Rapamycin induces tumor-specific thrombosis via tissue factor in the presence of VEGF. Blood 2005, 2004-2009-3540.
[22] Butzal M, Loges S, Schweizer M, Fischer U, Gehling UM, Hossfeld DK, et al. Rapamycin inhibits proliferation and differentiation of human endothelial progenitor cells in vitro. Exp Cell Res 2004;300:65–71.
[23] Sawyers CL. Will mTOR inhibitors make it as cancer drugs?. Cancer Cell 2003;4:343–348.
[24] Tsutsumi N, Yonemitsu Y, Shikada Y, Onimaru M, Tanii M, Okano S, et al. Essential role of PDGFalpha-p70S6K signaling in mesenchymal cells during therapeutic and tumor angiogenesis in vivo. Circ Res 2004;94:1186–1194.
[25] Patan S, Munn LL, Jain RK. Intussusceptive microvascular growth in a human colon adenocarcinoma xenograft: a novel mechanism of tumor angiogenesis. Microvasc Res 1996;51:260–272.
[26] Patan S, Tanda S, Roberge S, Jones RC, Jain RK, Munn LL. Vascular morphogenesis and remodeling in a human tumor xenograft: blood vessel formation and growth after ovariectomy and tumor implantation. Circ Res 2001;89:732–739.
[27] Djonov V, Andres AC, Ziemiecki A. Vascular remodelling during the normal and malignant life cycle of the mammary gland. Microsc Res Tech 2001;52:182–189.
[28] Guba M, Koehl GE, Neppl E, Doenecke A, Steinbauer M, Schlitt HJ, et al. Dosing of rapamycin is critical to achieve an optimal antiangiogenic effect against cancer. Transpl Int 2005;18:89–94.
[29] Abraham RT. mTOR as a positive regulator of tumor cell responses to hypoxia. Curr Top Microbiol Immunol 2004;279:299–319.
[30] Byrne AT, Ross L, Holash J, Nakanishi M, Hu L, Hofmann JI, et al. Vascular endothelial growth factor-trap decreases tumor burden, inhibits ascites, and causes dramatic vascular remodeling in an ovarian cancer model. Clin Cancer Res 2003;9:5721–5728.
[31] Mesiano S, Ferrara N, Jaffe RB. Role of vascular endothelial growth factor in ovarian cancer: inhibition of ascites formation by immunoneutralization. Am J Pathol 1998;153:1249–1256.